IOP Conf. Series: Materials Science and Engineering **152** (2016) 012048 doi:10.1088/1757-899X/152/1/012048

Experimental study on energy absorption of foam filled kraft paper honeycomb subjected to quasi-static uniform compression loading

N Abd Kadir, Y Aminanda*, M S Ibrahim and H Mokhtar

Mechanical Engineering Department, Faculty of Engineering,
International Islamic University Malaysia, 53100 Kuala Lumpur, Malaysia

*yulfian@iium.edu.my

Abstract. A statistical analysis was performed to evaluate the effect of factor and to obtain the optimum configuration of Kraft paper honeycomb. The factors considered in this study include density of paper, thickness of paper and cell size of honeycomb. Based on three level factorial design, two-factor interaction model (2FI) was developed to correlate the factors with specific energy absorption and specific compression strength. From the analysis of variance (ANOVA), the most influential factor on responses and the optimum configuration was identified. After that, Kraft paper honeycomb with optimum configuration is used to fabricate foam-filled paper honeycomb with five different densities of polyurethane foam as filler (31.8, 32.7, 44.5, 45.7, 52 kg/m^3). The foam-filled paper honeycomb is subjected to quasi-static compression loading. Failure mechanism of the foam-filled honeycomb was identified, analyzed and compared with the unfilled paper honeycomb. The peak force and energy absorption capability of foam-filled paper honeycomb are increased up to 32% and 30%, respectively, compared to the summation of individual components.

1. Introduction

Honeycomb sandwich structure has been used extensively as an energy absorber or a cushion to resist external loads due to its lightweight and high energy absorbing capability. However, its weakness due to impact loading, hygro-thermal and others becomes a significant preoccupation for its application in the industry. Extensive work has been carried out on the structural and failure behavior of honeycomb sandwich structure. Aktay *et al.* [1] developed several numerical techniques for modeling transverse crush behavior of honeycomb core materials and compared with test data on aluminum and Nomex honeycomb. Ajdari *et al.* [2] investigated in-plane dynamic crushing of two dimensional honeycombs with both regular hexagonal and irregular arrangements. Furthermore, the critical buckling loads for various core densities and materials of honeycomb composite panels were studied both experimentally and analytically by Kaman *et al.* [3]. In addition, Zhang *et al.* [4] investigated the crashworthiness of kagome honeycomb sandwich cylindrical column under axial crushing loads and presented the new type of kagome honeycomb sandwich in order to expand the plastic deformation zones and improve the energy absorption efficiency.

Petrone *et al.* [5] reported that energy absorption in honeycomb cores is minimally dependent on the height of the cell walls but predominantly dependent on geometrical parameters of the honeycombs,

essentially the cell wall thickness-to-length ratio (t/l) or the relative density of the core. In the case of compressive loads, the critical buckling load is dependent on the bending of the cell wall that is related by (t/l^3). Therefore, by increasing the relative density of the core, an increase of energy absorption in these cores can be expected. In addition, Xu *et al.* [6] reported that cell wall thickness to edge length ratio, t/l also plays the dominant role in the dynamic properties of honeycomb materials. In their work on the experimental study of out-of-plane dynamic compression of hexagonal honeycombs, they found that the tangent modulus increased towards the end of the crushing process, especially for honeycombs with small values of wall thickness to edge length ratio (t/l). For large cell size honeycombs, the plastic buckling is more likely to occur in the middle region of the specimens under quasi-static and dynamic compression, indicating that the deformation pattern is influenced by the dimension of the honeycomb cells. Other noteworthy studies on the effect of parameters of honeycomb on the energy absorption capability include Zhang *et al.* [4], Alavi and Sadegia [7] and Dongmei Wang [8].

The compression deformation behavior of polymer foam is one of the characteristics that make the material desirable in energy absorption applications. In particular, the ability of the foam to undergo large amounts of plastic deformation at nearly constant stress is advantageous. Therefore, polymeric foams have been investigated extensively as fillers for hollow cores [7, 9–11]. The results have shown that these low density foams have positive effect on strengthening the cell walls of panel and also has been credited with improving energy absorption capability and damping properties of the honeycombs [10, 12–13]. Alavi and Sadega [7] found that foam filling of hexagonal cell can increase their mean crushing strength and energy absorption capability up to 300%. In addition, the mean crushing strength of foam filled panel is always greater than summation of individual component. Aktay *et al.* [14] also reported that the restraining effect of filler shifted the deformation mode of Al tube from diamond to concertina in larger diameter tube. Besides, energy absorptions in foam-filled tube were increased with increasing filler density and higher than the summation of the energy absorption of empty tube (alone) and filler (alone).

In this research, honeycomb structure made from Kraft paper for load bearing application was used and manufactured manually in order to obtain the desired thickness, density and cell size. Optimum configuration of the unfilled Kraft paper honeycomb on both specific energy absorption and specific compressive strength was determined through statistical analysis of variance (ANOVA). Then, Kraft paper honeycomb with optimized parameters was filled with low density polyurethane foam in order to strengthen the cell walls. Series of quasi static experimental tests were carried out to investigate the force and specific energy absorption capability of foam filled kraft paper honeycomb.

2. Experiment materials and methods

2.1. Materials

The kraft paper honeycomb was fabricated from commercial kraft paper with three different densities (80gsm, 120gsm, 175 gsm) by using handmade honeycomb maker. The kraft paper honeycomb were coated with resin and cured at room temperature for 24 hours. Polyurethane foam were used as filler in the kraft paper honeycomb structure and it was made by mixing polyol and isocyanate in liquid foam. Five different types of polyol were used to produce five different density of polyurethane. However, only one type of isocyanate was used namely Maskiminate 80. The type of polyol and density of foam are shown in Table 1.

2.2. Design of experiment method

The full factorial design using Design-Expert Software was used to evaluate the effect of factors and to obtain the optimum configuration of Kraft paper honeycomb on specific energy absorption (SEA) and specific compressive strength(SCS). Full factorial design is a collection of statistical and mathematical techniques that are useful for the modeling and analyzing problems in which a response of interest is influenced by several variables and the objective is to optimize this response [15].

Table 1. Foam density and polyol type of polyurethane foam

Polyol type	Foam density (kg/m^3)
788B/4x2	31.8
788B/8	32.7
788B/2	44.5
788B/9/45	45.7
788B/9/68	52.0

Design-Expert software fitted four models; linear, two-factor interaction (2FI), quadratic and cubic polynomials to the responses and displayed a measure of progress during calculation. Linear models are generally used in most studies to assess the independent and dependent factors. In this model, the behavior of the dependent variables (response) can be expressed as Equation 1 [15].

$$y_i = \beta_o + \sum_{j=1}^{n} \beta_j X_{ij} + \varepsilon_i \quad (1)$$

where ε_i is independent random variables, β_o is the mean of observations, β_j is unknown constant, J is the factor and n is the number of observations.

The non-linear models are important and necessary to consider an experimental design that allows one to fit the experimental data to quadratic model. The general model presented in Equation 2 is used to describe the non-linear model [15].

$$y = \beta_o + \sum_{j=1}^{n} \beta_i X_i + \sum_{j=1}^{n} \beta_{ii} X_i^2 + \sum_{i=1}^{n} \sum_{i<j=2}^{n} \beta_{ij} X_i X_j \quad (2)$$

2.3. Foam filled kraft paper honeycomb

The Kraft paper honeycomb with the optimized configuration is used to fabricate the foam-filled Kraft paper honeycomb by using dipping process. The dipping process gave a uniform foam-filling inside the honeycomb cell for bigger cell size, hence this method is more practical manufacturing process in comparison to foam injection as proposed by [12]. The foam-filled paper honeycombs were subjected to quasi-static compression loading by using SHIMADZU Autograph AG-X 250 compression machine. The bottom plate was fixed and the upper plate was subjected to vertical downward displacement up to 22.5mm (50% of the honeycomb height) with a displacement rate of 0.5 mm/min. The force acting on the specimens was measured by load cell and force-displacement curve was plotted for further analysis.

3. Results and discussion

3.1. Analysis of design of experiment of unfilled kraft paper honeycomb

Analysis of variance (ANOVA) was conducted on the collected data to investigate the main effects of density of paper (*A*), thickness of cell (*B*) wall and also cell size of honeycomb (*C*), with three level interaction effects on the specific energy absorption (SEA) and specific compression strength (SCS). Table 2 shows the factors and levels of kraft paper honeycomb. The height for all specimens was 45mm. According to full factorial design method, 27 configurations of kraft paper honeycomb are generated considering three factors with three levels and the experimental results are shown in Table 3.

Table 2. The three factors and their levels

Factor	Code	Unit	Level 1	Level 2	Level 3
Density of paper	A	gsm	80	120	175
Thickness of cell wall	B	ply	1	2	3
Cell size of honeycomb	C	mm	10	15	20

Table 3. The experimental results obtained based on full factorial design

Run	*A*	*B*	*C*	Specific compression strength (Mpa/kg)	Specific energy absorption (J/kg)
1	175	2	10	16.79	1128.41
2	80	2	20	9.25	657.42
3	80	2	10	23.10	535.93
4	120	3	15	6.69	203.55
5	175	3	20	7.64	808.94
6	80	3	15	3.50	71.69
7	120	2	10	12.79	325.15
8	120	1	20	7.87	436.98
9	120	2	15	14.48	458.22
10	120	3	10	15.59	270.64
11	80	1	20	1.70	81.09
12	80	3	20	6.06	426.57
13	175	2	20	4.09	452.96
14	80	1	10	7.59	97.67
15	175	1	20	7.09	560.30
16	175	2	15	11.16	647.34
17	120	1	10	14.91	266.13
18	120	1	15	16.69	421.35
19	80	2	15	16.44	595.467
20	80	3	10	22.15	569.33
21	175	1	10	17.50	559.68
22	120	3	20	4.87	332.11
23	175	3	20	9.50	661.96
24	175	1	15	8.02	337.70
25	120	2	20	6.06	472.63
26	175	3	10	13.422	601.65
27	80	1	15	7.29	335.18

3.1.1. Analysis of specific energy absorption. According to the sequential model sum of squares, the models were selected based on the highest order polynomials where the models were not aliased and the additional terms were significant. From the analysis, it found that the two-factor interaction model come out the best for specific energy absorption (SEA). This is because it exhibits a high R-square values of 0.8496. The predicted R-square of 0.5717, is in reasonable agreement with adjusted R-square of 0.7556. Adequate precision measures the signal to noise ratio and the ratio greater than 4 is desirable. The ratio for SEA is 11.819 and this indicates that an adequate signal and model can be used to navigate the design space.

The result of ANOVA analysis for SEA is presented in Table 4. For each response, the probability (Prob>F) was examined to check if it falls below 0.05. The model for SEA was developed with 99% confident level and P-value less than 0.001, which indicates that this model are highly significant. *A, B*

and *C* refers to density of paper, thickness of cell wall and cell size of honeycomb, respectively. Based on the P-value, density of paper, thickness of cell wall and cell size of honeycomb were found to have significant effect on SEA. Values greater than 0.1000 indicate the model terms are not significant.

The F-value for each factor is simply a ratio of the mean of squared deviations to the mean of the squared errors. A larger F-value means that the factor has greater significance for SEA. From Table 4, it reveals that thickness of cell wall, *B* as most significant factor with F-value of 24.10, followed by density of paper, *A* and cell size of honeycomb, *C* with F-value of 12.13 and 4.77, respectively. The F-value for interaction between density of paper, *A* and cell size of honeycomb, *C* is 2.10, which implies a weak influence of the two factor interaction to SEA value. The two-factor interaction model for SEA is given in Equation 3.

$$SEA= 426.33 - 105.03A_1 + 27.55A_2 - 145.94B_1 + 31.68B_2 + 62.86\ C_1 - 8.35C_2 + 6.10A_1C_1 - 49.93A_2C_1 - 55.27A_1C_2 + 21.03A_2C_2 \quad (3)$$

Table 4. Analysis of variance (ANOVA) for SEA

Source of data	Sum of square	Degree of freedom	Mean square	*F* value	Prob >*F*	Comment
Model	5.967E+005	10	59669	9.04	<0.0001	Significant
A	1.602E+005	2	80077.86	12.13	0.0006	
B	3.182E+005	2	1.591E+005	24.10	<0.0001	
C	62932.46	2	31466.23	4.77	0.0238	
AC	55395.17	4	13848.79	2.10	0.1287	

3.1.2. Analysis for specific compressive strength. Similarly, the best model for specific compressive strength (SCS) is two-factor interaction (2FI). This is due to low standard deviation (Std. Dev) of 0.75, high R-square value of 0.9390 and a low PRESS value of 34.61. The predicted R-square of 0.6912 is in reasonable agreement with adjusted R-square of 0.8678. The adequate precision is 15.95, which indicates that a satisfactory signal and model can be used to navigate the design. Table 5 summarizes the result of ANOVA analysis for SCS. The same parameters have been used for SEA analysis previously. Density of paper, thickness of cell wall and cell size of honeycomb were found to have significant effect on SCS with P-value 0.05. Thickness of cell wall resulted as most significant parameter for SCS with F-value of 48.91, followed by density of paper and honeycomb cell size with the F-value of 17.03 and 16.66, respectively. The lower F-value for interaction between AB and BC implies weak interaction between these parameters. The proposed models for SCS is expressed in Equation 4.

$$SCS = 6.08 - 1.19A_1 + 0.49A_2 - 1.92B_1 + 0.40B_2 + 1.12C_1 - 0.23C_2 - 0.100A_1B_1 - 0.54A_2B_1 + 0.15A_1B_2 - 0.15A_2B_2 - 0.18B_1C_1 - 0.38B_2C_1 + 0.66B_1C_2 + 0.20B_2C_2 \quad (4)$$

Table 5. Analysis of variance (ANOVA) for SCS

Source of data	Sum of square	Degree of freedom	Mean square	*F* value	Prob >*F*	Comment
Model	105.23	14	7.52	13.19	<0.0001	Significant
A	19.43	2	9.73	17.08	0.0003	
B	55.73	2	27.86	48.91	<0.0001	
C	18.98	2	9.49	16.66	0.0003	
AC	4.94	4	1.23	2.17	0.1348	
BC	6.12	4	1.53	2.69	0.0827	

3.1.3. Optimization parameter of kraft paper honeycomb. The density of paper, thickness of cell wall and cell size of honeycomb were found to have significant effect on SEA and SCS. Both SEA and SCS were found to increase with decreasing of honeycomb cell size and increasing of density of paper and thickness of cell wall. The trend was agreed with other researchers who found that the higher cell wall thickness and smaller cell size increase the energy absorption and crush strength [6, 16]. The highest value of responses were obtained when honeycomb cell size at minimum point, while density of paper and thickness of cell wall at maximum point within the range of study. As a result, it was found that the optimum configuration of the unfilled Kraft paper honeycomb on SEA and SCS within the range of this study is: kraft paper density of 175 gsm, cell wall thickness of 3 ply and honeycomb cell size of 10mm.

3.2. Unfilled kraft paper honeycomb

The force-displacement curves of selected kraft paper honeycomb compressed to the 50% deformation in quasi static compression are shown in Figure 1. The graphs show that there is elastic behavior at the beginning of the indentation until a critical load is reached. Then, sharp drop is observed after the peak load, which corresponds to the beginning of the vertical edge deformation. The force then decreases to reach a plateau, which corresponds to the succession of fold forming and ends up by condensation of the honeycomb [17]. The deformation of selected kraft paper honeycomb of paper can be observed in Figure 2.

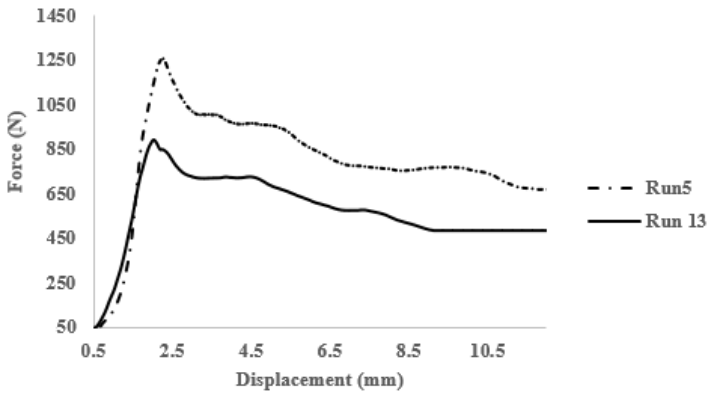

Figure 1. Force-displacement curves of selected kraft paper honeycomb

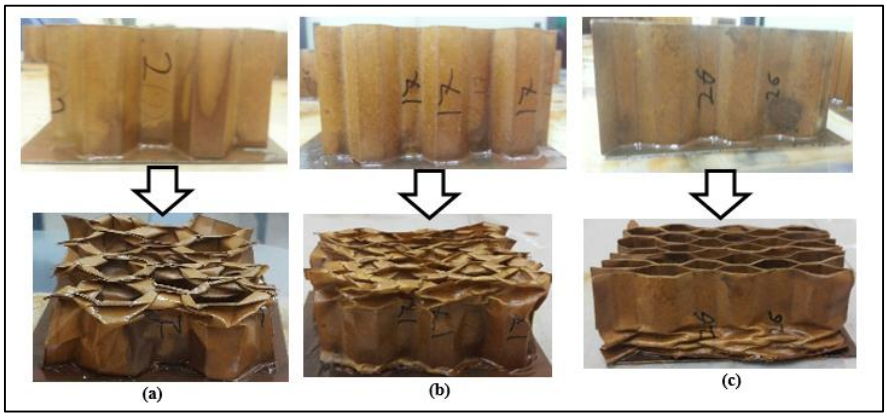

Figure 2. Condition of selected kraft paper honeycomb before (top) and after (bottom) quasi static compression test

The failure mechanism of kraft paper honeycomb consists of buckling of the cell walls and vertical edges, wall buckling on the top or bottom surfaces and the tendency of unstable outer cells to buckle

towards inward or outward direction. Initially, as kraft paper honeycomb was compressed, the lower part of the cell walls started to buckle. The cell walls started to buckle locally at the weakest point along the height, which is the bottom part of the structure. This lower part of cell walls continued to buckle as the kraft paper honeycomb was compressed further. Then, the number of folds of walls and vertical edges increased until reaching the densification phase. It is also can be observed from Figure 2 that the kraft paper honeycomb with 3 ply of thickness of paper (c) buckled only on the top surface compare to 1 ply (b) and 2 ply (a), where the wall buckling on both side of honeycomb. This condition happened due to the imperfections of the cell alignment during the manufacturing process. However, the fold shape is same for all samples. The folding mechanism is similar to Nomex honeycomb that reported by Aminanda *et al.* [1].

3.3. Foam-filled kraft paper honeycomb structure

The Kraft paper honeycomb (Figure 3a) with optimized configuration (175gsm, 3ply, 10mm) was used to fabricate the foam-filled Kraft paper honeycomb (Figure 3b). Five different densities of foam was used with its identification using FFP1 to FFP5 respectively with increase of foam density. The list of the five different densities of foam and its designation are shown in Table 6.

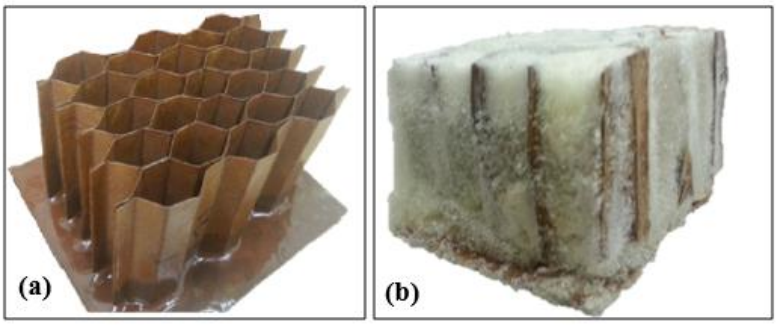

Figure 3. Condition of (a) unfilled kraft paper honeycomb (b) foam-filled kraft paper honeycomb

Table 6. Foam density and designation of foam-filled kraft paper honeycomb

Designation	Foam density (kg/m^3)
FFP1	31.8
FFP2	32.7
FFP3	44.5
FFP4	45.7
FFP5	52.0

The force in function of the compression displacement for all specimens are drawn in Figure 4. The shape of the curves is almost similar with that of unfilled kraft paper honeycomb. However, the peak load of the foam-filled kraft paper honeycomb is broader than unfilled honeycomb, which is due to the foam occupied at the fold angle that gives a higher residual resistance and less abrupt behavior. From the graph, the energy absorption were determined by measuring the net area under force-displacement curve and it was measured until 22.5mm. Meanwhile, peak force was obtained by taking the maximum force of each curves. Table 7 and Table 8 represent the comparison of energy absorption capability and peak forces between the foam-filled Kraft Paper honeycombs and the summation of their individual components. The specific energy of individual component were calculated using Equation 5.

$$SEA_{f+h} = \frac{E_f + E_h}{m_f + m_h} \quad (5)$$

where E_f and E_h, are energy absorption for foam and honeycomb, while m_f and m_h are mass for foam and honeycomb, respectively. Meanwhile, specific energy absorption of foam-filled were calculated using Equation 6.

$$SEA_{ff} = \frac{E_{ff}}{m_{ff}} \tag{6}$$

where E_{ff} is energy absorption for foam-filled, while m_{ff} is mass for foam-filled. Since the total mass of individual element is almost the same as compared to that of the foam-filled honeycomb, the energy absorption increment relates also to the specific energy absorption.

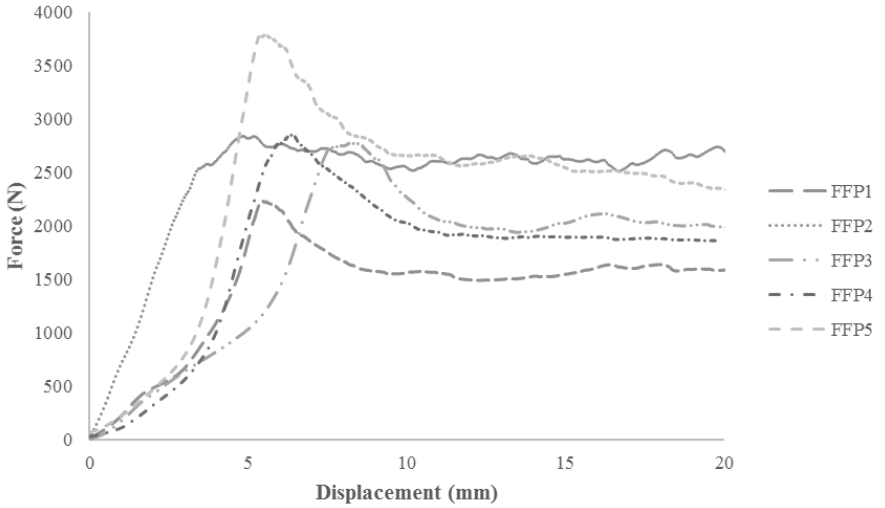

Figure 4. Force-displacement curves of foam-filled with five densities of foam

Table 7. Comparison of energy absorption capabilities between foam filled paper honeycomb and summation of its individual component

Foam-filled honeycomb	Energy absorbed (J)				
	Unfilled paper honeycomb (a)	Polyurethane foam (b)	Summation (a) + (b)	Foam-filled paper honeycomb	% Increase
FFP1	24.56	5.87	30.43	32.19	5.78 **%**
FFP2		7.81	32.37	38.75	19.70 %
FFP3		9.00	33.56	33.92	1.07 %
FFP4		12.97	37.53	48.93	30.38 %
FFP5		17.85	42.41	55.03	29.76 %

Table 8. Comparison of peak forces between foam filled paper honeycomb and summation of its individual component

Foam-filled honeycomb	Peak Force (kN)				
	Unfilled paper honeycomb (a)	Polyurethane foam (b)	Summation (a) + (b)	Foam-filled paper honeycomb	% Increase
FFP1	2.381	0.121	2.502	2.235	-10.67 %
FFP2		0.191	2.572	2.844	10.58 %
FFP3		0.247	2.628	2.780	5.78 %
FFP4		0.387	2.768	2.852	3.03 %
FFP5		0.490	2.871	3.796	32.21 %

From Table 7, it can be seen that energy absorbed of foam-filled honeycombs is always higher than the summation of their individual components. Foam-filled Kraft paper honeycomb with foam density 45.7 kg/m^3 (FFP4) shows the highest increment of energy absorbed with 30.38 % increase. It is also found that the percentage increase in SEA for higher density of foam filling (FFP4 and FFP5) are much higher compared to low density of foam (FFP1, FFP2, FFP3). This results also show agreement with study of Aktay *et al.* [14] that the energy absorption of foam-filled tube increases with increasing filler density and higher than the summation of the energy absorption of empty tube (alone) and foam filler (alone). Increment of energy absorption capability was due to the change of boundary condition on the top and bottom surfaces of the honeycomb from free-free to fixed-fixed boundary condition. The foam densification was found to occur at the buckled cell walls. This foam densification occurred due to the compression between one buckled wall and its neighboring walls. Therefore, after the sharp drop of force, the force fluctuated with number of wall buckling and densification of foam. As a results, the energy absorption capability of the foam-filled kraft paper honeycomb was increased and its values were higher than the summation of individual components.

Comparison of peak forces between foam-filled paper honeycomb in Table 8 shows that almost all peak force values of foam filled are higher than the summation of their individual component except for the peak force of foam-filled Kraft paper honeycomb with 31.8 kg/m^3 density of foam (FFP1). The Kraft paper honeycombed filled by the highest density of polyurethane foam (52 kg/m^3) displays the highest increment of peak force with 32.21% increases. The foam infill has increased the bending and buckling resistivity of the honeycomb core cell walls. Due to this support, the peak force is increased and the transmitted load from the front face to the back face is increased, although the foam inside the cell has not compressed to its maximum value.

The specific energy absorption of the foam-filled kraft paper honeycomb with different densities is plotted in Figure 5. From the graph, the optimum value of specific energy absorption is obtained at the maximum point of the specific energy absorption curve. It is found that the optimum specific energy absorption can be divided into two regions within the range of density studied for this work. For foam density less than 44.5 kg/m^3, the optimum SEA is found for foam density of 33 kg/m^3. As for density higher than 44.5 kg/m^3, more experiments needs to be performed to reach an eventual optimum SEA as shown in Figure 5. It is also noted that for lower density foam filling (less than 44.5 kg/m^3), it is almost ineffective to increase the SEA of foam-filled kraft paper honeycomb over unfilled kraft paper honeycomb.

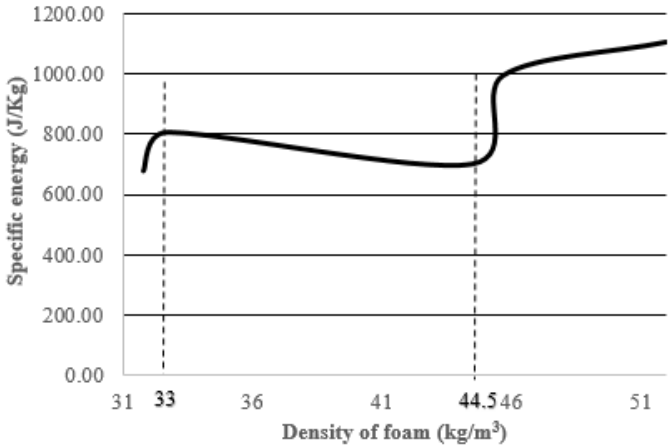

Figure 5. Specific energy absorption of foam-filled kraft paper honeycomb with different densities of foam

Failure mechanism of foam-filled paper honeycomb is comprised by interaction between cell walls and foam, where the foam filled up the folds. The condition of the foam filled kraft paper honeycomb before and after compression can be observed clearly in Figure 6 and Figure 7.

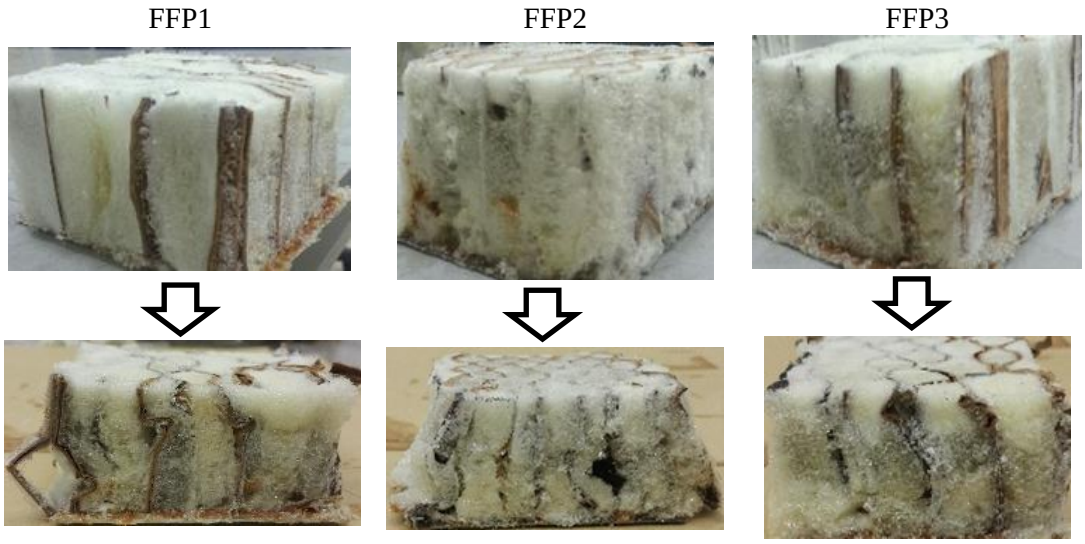

Figure 6. Condition of foam-filled kraft paper honeycomb before (top) and after (bottom) quasi-static compression test for FFP1, FFP2 and FFP3

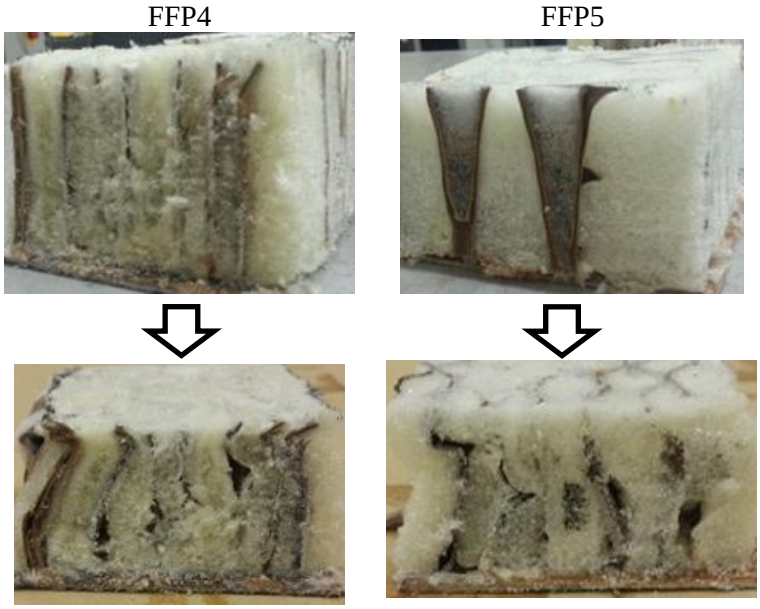

Figure 7. Condition of foam filled kraft paper honeycomb before (top) and after (bottom) quasi-static compression test for FFP4 and FFP5

The buckling of cell walls starting at the middle of the structure and followed by foam densification at the same location. As illustrated in the figures, the most obvious observation if compared to unfilled kraft paper honeycomb is the condition on the top and bottom surface of the structure. There is no buckling at the wall on the top and the bottom surfaces of kraft paper filled with polyurethane foam even though the specimens were compressed until densification phase. This is in contrast with unfilled kraft paper honeycomb, where the numbers of buckled wall on the surface increase as displacement increases. On the surface of foam-filled kraft paper honeycomb, the shape of multiple hexagonal tubes remains as hexagonal even though they were compressed until the densification phase. Therefore, it is found that the failure mode was changed from wall buckling on the top and bottom surface for unfilled

kraft paper honeycomb to the wall buckling on the middle of the structure for foam-filled kraft paper honeycomb.

The failure mechanism of foam-filled kraft paper honeycomb was divided into three stages: before plateau region, plateau region and end of plateau region. Before plateau region, the buckling of cell wall and vertical edge is less severe compared to unfilled kraft paper honeycomb and there is still no tearing of double thickness wall. In plateau region, the foam starts to push the bucked wall and filling the void between the folds. Tearing of cell wall occurs but pushed against each other. At the end of the plateau region, the whole cell wall bucked with bigger fold length compared to unfilled kraft paper honeycomb. The wall buckled at the middle of the structure, and no wall buckling at the upper and lower surface. It also can be seen clearly in Figure 6 that few outer cells buckled out since they were not supported from the outside and because they were only supported by three neighboring cells and only two for the cells at the end corners.

The failure behavior of the kraft paper honeycomb was found to be similar to foam-filled Nomex honeycomb that was reported by Wan *et al.* [12]. Based on the figures, it also shows a change of the boundary condition from free-fixed type (local buckling) of unfilled kraft paper honeycomb to fixed-fixed (global buckling) for foam-filled honeycomb subjected to compression loading. The change of the boundary conditions explains the peak force and energy absorption increment of the foam-filled honeycomb, together with the fact that the foam strengthens the honeycomb cell walls and cell walls confined the foam during the compression loading.

4. Conclusion

In conclusion, experimental design methodology has been shown to be a valuable tool to obtain the optimum configuration for kraft paper honeycomb and to explore the influences of density of paper, thickness of cell wall and cell sizes of honeycomb on the specific energy absorption and the specific compression stress. The results reveal that all factors give significant effect, however the thickness of cell wall has the most influence on the performance of kraft paper honeycomb. It is also found that the optimum configuration for kraft paper honeycomb is paper density of 175gsm, cell wall thickness of 3 ply and honeycomb cell size of 10mm. Besides, the kraft paper honeycomb is found to collapse by the buckling of cell walls and vertical edges on the top and bottom surfaces when they were compressed under quasi-static compression. The kraft paper honeycomb with the optimum configuration was filled up with low density polyurethane. The results reveal that filling the kraft paper honeycomb up with polyurethane foam does help strengthening its cell wall, hence improves the energy absorption and peak force of kraft paper honeycomb. This was proven experimentally where the energy absorption and peak force were found to be larger for foam-filled honeycomb structure in comparison to the summation of individual component while the total weight of components remains the same compared to foam-filled honeycomb. From the experimental observation, the increment of peak force and energy absorption is due to change of boundary conditions from free-fixed on honeycomb structure producing local buckling to fixed-fixed on foam-filled producing global buckling. In addition, the effect of foam in strengthening the cell walls and the effect of cell walls in confirming the foam contribute to the higher value of peak force and energy absorption of foam-filled honeycomb structure. Furthermore, the change of failure deformation from wall buckling on the top and bottom surface for unfilled kraft paper honeycomb to the wall buckling at the middle of the structure for kraft paper honeycomb filling with polyurethane foam is also noted.

Acknowledgements

This research was supported by Ministry of Higher Education Malaysia and Research Management Centre of the International Islamic University Malaysia (Grant no: FRGS14-155-0396)

References

[1] Aktay L, Johnson A F and Kröplin B-H 2008 *Eng. Fract. Mech.***75** 2616–30
[2] Ajdari A, Nayeb-Hashemi H and Vaziri A 2011 *Int. J. Solids Struct.* **48** 506–16

[3] Kaman M O, Solmaz M Y and Turan K 2010 *J. Compos. Mater.***44** 2819–31
[4] Zhang Z, Liu S and Tang Z 2010 *Thin-Walled Struct.* **48** 9–18
[5] Petrone G, Rao S, De Rosa S, Mace B R, Franco F and Bhattacharyya D 2013 *Compos. Struct.* **100** 356–62
[6] Xu S, Beynon J H, Ruan D and Lu G 2012 *Compos. Struct.* **94** 2326–36
[7] Alavi Nia A and Sadeghi M Z 2010 *Mater. Des.* **31** 1216–30
[8] Wang D 2009 *Int. J. Impact Eng.* **36** 110–4
[9] Burlayenko V N and Sadowski T 2010 *Compos. Struct.* **92** 2890–900
[10] Niknejad A, Liaghat G H, Moslemi Naeini H and Behravesh A H 2011 *Mater. Des.* **32** 69–75
[11] Vaidya U K, Ulven C, Pillay S and Ricks H 2003 *J. Compos. Mater.* **37** 611–26
[12] Wan Abdul Hamid W L H, Aminanda Y and Shaik Dawood M S I 2013 *Appl. Mech. Mater.* **393** 460–6
[13] Zhang G, Wang B, Ma L, Wu L, Pan S and Yang J 2014 *Compos. Struct.* **108** 304–10
[14] Aktay L, Toksoy A K and Gü Den M 2006 *Mater. Des.* **27** 556–65
[15] Douglas C. Montgomery 2001 *Design and analysis of experiments* (Hoboken: Wiley)
[16] Khoshravan M R and Najafi Pour M 2014 *Thin-Walled Struct.* **84** 423–31
[17] Aminanda Y, Castanié B, Barrau J-J and Thevenet P 2005 *Appl. Compos. Mater.* **12** 213–27